Materials Research. 2025; 28: e20240493
DOI: https://doi.org/10.1590/1980-5373-MR-2024-0493

Research on the Automatic Recognition Method of Micro-nano Regeneration Rubber Filler Dispersion in Scanning Electron Microscope Images

Yunhui Xu[a], Min Deng[a], Hui Tu[a]*, Zaheer ul haq[b], Haifeng Xu[c], Zhenghua Xin[c]

[a]Xuzhou College of Industrial Technology, School of Materials Engineering, Xuzhou, China.
[b]Shanghai Jiao Tong University, School of Chemistry and Chemical Engineering, Shanghai, China.
[c]Suzhou University, School of Information Engineering, Suzhou, China.

Received: October 30, 2024; Revised: May 09, 2025; Accepted: June 14, 2025

Micro-nano regenerative rubber represents a significant advancement over traditional regenerative rubber by eliminating the need for polluting chemical agents such as coal tar, asphalt, and regenerators. The performance of composite materials filled with micro-nano regenerative rubber depends critically on the degree of filler dispersion. However, current methods for assessing dispersion rely on subjective visual estimation of electron microscope images, which lack quantitative precision and are prone to human error, especially given the complex distribution of micro-nano particles. This study introduces a novel, automated method for grading the dispersion of micro-nano regenerative rubber fillers in scanning electron microscope (SEM) images, leveraging advanced image processing techniques. The proposed method automatically identifies and quantifies the dispersion of micro-nano regenerative rubber clusters through particle size and distribution analysis. By establishing objective grading rules for dispersion levels, it provides a reliable and efficient alternative to traditional subjective assessments. This innovative approach not only enhances the accuracy of dispersion evaluation but also facilitates the development of high-performance composite materials by enabling precise control over filler distribution. The method's effectiveness is validated through comprehensive experimental analysis, demonstrating its potential to significantly improve the quality and consistency of micro-nano regenerative rubber applications in various industries.

Keywords*: Micro-nano regenerative rubber, Scanning electron microscopy (SEM), Dispersion, Image processing.*

1. Introduction

Regenerative rubber is obtained from waste rubber products through physical or chemical treatment methods. The use of regenerative rubber as a filler can significantly reduce the dependence on virgin rubber and decrease the consumption of natural resources[1]. Compared to virgin rubber, the cost of regenerative rubber is typically lower, and using it as a filler can reduce material costs and enhance the competitiveness of products[2,3]. On the other hand, by recycling and reusing waste rubber, the use of regenerative rubber filling helps to mitigate the environmental impact of landfilling and incineration, reduces the consumption of energy, water resources, and chemicals associated with the production of virgin rubber, and facilitates the resource utilization of waste, aligning more with current concepts of environmental protection and sustainable development[4,5]. The use of regenerative rubber contributes to promoting a more green, low-carbon, and sustainable circular economic development model[6].

Unlike traditional regenerative rubber, micro-nano regenerative rubber is produced using an air oxidation method without the addition of chemical materials such as coal tar, asphalt, and regenerators. On one hand, this can further reduce the negative impact on the environment during the preparation process. On the other hand, the particle size of micro-nano regenerative rubber typically reaches nano or micro scales, with small particle size and large surface area. Therefore, they have better interfacial compatibility with the matrix material[7]. This fine microstructure provides higher uniformity and stability during filling and compounding processes, helping to reduce interfacial defects and further improve the performance of composite materials, such as enhancing strength, toughness, and wear resistance[8]. Due to its excellent performance and environmental friendliness, micro-nano regenerative rubber has a broader application prospect. It can be used to manufacture various rubber products, tires, soles, seals, etc., to meet the material performance needs of different industries[9].

The degree of dispersion of regenerative rubber fillers is extremely important[10,11]. When the dispersion of micro-nano regenerative rubber is high, meaning the fillers are evenly distributed within the matrix material without aggregation, it can effectively enhance the mechanical properties of the composite materials, such as tensile strength, tear strength, and wear resistance[12]. At the same time, the interface bonding strength between the fillers and the matrix material in the composite material is strong, effectively resisting the erosion

*e-mail: 495816333@qq.com
Associate Editor: Rodrigo Orefice
Editor-in-Chief: Luiz Antonio Pessan

and destruction of the external environment, and extending the service life of the composite material[13]. Conversely, if the dispersion is low and the fillers are unevenly distributed within the matrix material, stress concentration points are likely to form, leading to a decrease in the mechanical properties of the composite material. Weak interface bonding allows the composite material to be easily affected by the external environment, resulting in a shortened service life. During electron microscopy scanning imaging of micro-nano regenerative rubber filling, clustered structures can be observed[14], The dispersibility of fillers plays an important role in strengthening structures[15], but the scanning does not generate corresponding dispersion grades. Currently, there is relatively little research on the dispersion of micro-nano regenerative rubber filling, and relying on subjective human observation is not effective in distinguishing dispersion grades. Based on the above research motivation, an automated dispersion grading method based on image processing technology has been developed.

Chang et al.[16] investigated the influence of magnetic particle dispersion on the magnetic properties in composite magnetic films fabricated with a polymer substrate. By using silane coupling agents and oleic acid to enhance dispersion, they achieved improved visual dispersion in SEM images and enhancement of magnetic permeability. Li et al.[17]. designed a function named PDF (Particle Distribution Function) to quantify the dispersion state of fillers in images. The PDF evaluates filler density and determines local dispersion by analyzing density distribution. However, this method is sensitive to noise and risks misidentification for non-particulate fillers. While effective on simulated images, it has not been validated in real-world scenarios. Xu et al.[18]. studied the Payne effect of carbon black in natural rubber composites. They explored the rheological recovery capability of compounds under varying dispersion states of carbon black aggregates observed in SEM images. Łapińska et al.[19]. argued that insufficient uniformity of fillers in nanocomposites compromises the performance of high-concentration filler materials. They employed magnetic mixer stirring, calendering, and microfluidic techniques to disperse graphene fillers in nanocomposites. Using polarized interference microscopy, scanning electron microscopy, and Raman imaging spectroscopy, they analyzed how filler dispersion affects PDMS chain mobility, crosslinking density, grain size, and defect density, further influencing material performance.

Demir et al.[20] applied hierarchical clustering to microscope images to measure the Euclidean distance between particles. By comparing interparticle distances to a critical threshold, they determined the dispersion or agglomeration state of fillers. These distances were used to generate histograms and fitted to normal distributions to assess dispersion. Ref[21]. reviewed filler dispersion in energy-storage composites and simulated dielectric properties under different dispersion states and filler-interface models. Ref[22]. achieved well-dispersed polypropylene composites using fluorescence labeling and surface organic modification for inorganic fillers. Laser scanning confocal microscopy visualized the materials, and fractal dimension analysis quantified dispersion. Subsequent experiments confirmed correlations between dispersion and mechanical performance.

Proposed an automated method for assessing the dispersion of regenerated rubber fillers based on scanning electron microscopy (SEM) images. This method employs image enhancement, binarization processing, and an equivalent agglomeration conversion algorithm to achieve quantitative analysis of micro-nano regenerated rubber filler dispersion. By establishing objective grading criteria (Level value) based on pixel ratios and the proportion of small particles, it replaces traditional subjective evaluations reliant on human judgment, significantly improving the accuracy and reproducibility of results. Experimental data confirm that dispersion exhibits a strong positive correlation with key mechanical properties of the material, such as tensile strength, elongation at break, and tear strength (Pearson correlation coefficient up to 0.938), and reveals the direct impact of dispersion on vulcanization performance (e.g., t90 time). Unlike existing methods (e.g., fluorescence labeling) that require complex preprocessing and are unsuitable for industrial applications, this approach enables large-scale analysis of high-resolution SEM images without additional labeling or specialized equipment, offering a practical and efficient solution for industrial scenarios. The main contributions of this article are as follows:

(1) A novel automated method for quantifying filler dispersion in SEM images;
(2) Objective grading rules replacing subjective human judgment;
(3) Demonstrated correlations between dispersion and mechanical properties."

2. Experiment

2.1. Experimental formulation

The rubber material used in the experiment was primarily processed using an XK-160 mill for mastication and mixing. The mixing was carried out using a two-stage mixing method. The first stage of mixing mainly involved the preparation of masterbatch rubber excluding sulfur, accelerators, and micro-nano regenerative rubber, by mixing standard rubber 20#, Chlorinated butyl rubber 1240, and other compounding agents. This masterbatch was then stored for 8-48 hours. The second stage of mixing primarily involved the preparation of the final rubber compound by mixing the masterbatch with sulfur, accelerators, and micro-nano regenerative rubber, followed by storage for 8-48 hours. The formulations are presented in Table 1, where each formulation is identical except for the varying content of micro-nano regenerative rubber. The micro-nano regenerated rubber used in this study was developed by our research group. It is derived from truck tire rubber powder, primarily composed of tread rubber with NR (Natural Rubber) 60 phr and BR (Butadiene Rubber) 40 phr. Detailed information is provided in Ref[23].

Raw Materials: Standard Malaysian Rubber (SMR-20) (NR) and Chlorinated Butyl Rubber (ClR) 1240 were supplied by Shanghai Fenglu Chemical Co., Ltd.Micro-nano reclaimed rubber was a self-developed product.Carbon Black N330 was purchased from Hebei Daguangming Industrial Group (Damei Carbon Black Co., Ltd.). Other compounding agents: Zinc oxide, stearic acid, magnesium oxide, aromatic

Table 1. Ingredients List(Unit:phr).

Material name	1#	2#	3#	4#	5#	6#	7#	8#
20# standard adhesive	10	10	10	10	10	10	10	10
Chlorinated butyl rubber 1240	90	90	90	90	90	90	90	90
1# Micro Nano Recycled Rubber	20	25	35	40	45	50	55	60
Stearic acid	2	2	2	2	2	2	2	2
Magnesium oxide	0.5	0.5	0.5	0.5	0.5	0.5	0.5	0.5
Pottery clay	20	20	20	20	20	20	20	20
High abrasion furnace black N330	40	40	40	40	40	40	40	40
Protective wax	1	1	1	1	1	1	1	1
Aromatic oil	4	4	4	4	4	4	4	4
Rosin	1	1	1	1	1	1	1	1
Zinc oxide	10	10	10	10	10	10	10	10
Accelerator TMTD	1	1	1	1	1	1	1	1
Accelerator DM	1	1	1	1	1	1	1	1
Sulfur	1.9	1.9	1.9	1.9	1.9	1.9	1.9	1.9
Total	200.5	205.5	215.5	220.5	225.5	230.5	235.5	240.5

oil, rosin, accelerator TMTD, accelerator DM, protective wax, and sulfur were commercial-grade products.

Experimental Equipment: Model 660-1 single-blade rubber cutter: Wuxi First Rubber & Plastic Machinery Co., Ltd.Electronic balance (Model 0768#): Zhejiang Junkai Shun Industry & Trade Co., Ltd.X(S)M-1/20-80 internal mixer and XK-360 open mill: Wuxi First Rubber & Plastic Machinery Co., Ltd. YXE-25D flat vulcanizing press: Shanghai Xima Weili Rubber & Plastic Machinery Co., Ltd.FEI Teneo VS scanning electron microscope (SEM) and ACE600 vacuum coater: Leica Microsystems Inc. Disper aView carbon black dispersion analyzer: ALPHA Technologies (USA). GT-M2000-A rotorless curemeter, GT-7016 sample cutter, GT-AI-7000-GD electronic tensile tester, GT-7017-EMI thermal aging oven, and RH-2000N compression heat buildup tester: Gaotie Testing Instruments Co., Ltd. GTR-701B gas barrier tester: Jinan Sike Testing Technology Co., Ltd.

Experimental Methods and Conditions:

(1) Vulcanization Property Testing and Experimental Conditions(1) Vulcanization Property Testing and Experimental Conditions

Vulcanization characteristics were tested in according to ISO 6502:1991[24] «Rubber—Measurement of vulcanization characteristics with rotorless curemeters.»Oscillation frequency: 1.7 Hz ± 0.1 Hz. Amplitude: 1.00° ± 0.02°. Temperature: 160°C. Pressure: ≥8 kN.

(2) Dispersion Testing Method and Conditions

Filler dispersion was evaluated following ASTM D7723-11[25] «Standard Test Method for Rubber Property—Macro-Dispersion of Fillers in Compounds.» Test specimens were sectioned with a razor blade. Agglomerates, Filler clusters bound by van der Waals forces (carbon black) or hydrogen bonding (silica). Macro-dispersion: Distribution of fillers in compounds, typically in the micron range (2–100 μm).

(3) Mechanical Property Testing and Conditions

Mechanical property testing of rubber materials: According to GB/T 528-2009[26] "Determination of tensile stress-strain properties of vulcanized rubber or thermoplastic rubber", the experimental testing speed is 50 mm/min; The sample is a dumbbell shaped Type 1 sample, with a working length of 25 ± 0.5 mm, a thickness of 2.00 ± 0.2 mm, and a width of 6.00 ± 0.1 mm.

(4) Tear Strength Testing and Conditions

The tear strength of the rubber material is determined according to GB/T 529-2008[27] "Determination of Tear Strength of Vulcanized Rubber or Thermoplastic Rubber". The sample is a right angled sample with a minimum length of 100mm, a width of 19 ± 0.05 mm, and a sample angle of 90 °.

(5) Aging Performance Testing and Conditions

Thermal oxidative aging resistance was tested per GB/T 3512-2014[28] «Vulcanized rubber or thermoplastic rubber—Accelerated aging and heat resistance tests.» Aging temperature: 100°C. Aging time: 72 h.

(6) Compression Heat Buildup Testing and Conditions

Heat generation under compression was evaluated using ISO 4666-3:2010[29] «Rubber, vulcanized—Determination of temperature rise and resistance to fatigue in flexometer testing—Part 3: Compression flexometer (constant-strain type).» Stroke: 5.71 ± 0.03 mm. Frequency: 30 ± 0.3 Hz. Preload: 1.00 ± 0.03 MPa. Temperature: 55°C. Duration: 25 min.

(7) Gas Barrier Property Testing and Conditions

Gas permeability was measured according to ISO 2782:1995[30] «Rubber, vulcanized or thermoplastic—Determination of permeability to gases.» The airtightness of vulcanized rubber is determined using the constant pressure method. The sample size is 150mm x 95mm x 2mm, with a clean surface and no bubbles. The test gas is ammonia gas, with an experimental pressure difference of 0.101 ± 0.001MPa and an experimental temperature of 23 ± 2 °C.

2.2. Preparation of micro-nano recycled rubber

Put 40kg truck tire rubber powder (Ground tire rubber: GTR for short) in 200L self-designed tank-type thermal oxidative degradation equipment, pass into the pulse air with adjustable flow rate, and get different degradation degree of regenerated rubber through the regulation of the thermal oxidative degradation reaction time at 200°C, and after the thermal degradation reaction time of 10min to produce the MOMN-RGTR material. The homemade thermal oxidation

reactor is shown in Figure 1a is the equipment diagram, (b) is the equipment structure schematic diagram.

2.3. Morphological characterization of filled micro nano regenerated rubber vulcanized rubber

Experimental instruments: The instruments used were scanning electron microscope FEI Teneo VS and vacuum deposition instrument ACE600, Leica MicrosystemsInc.

Method principle: Electrons are emitted from an electron gun and gradually converged by a condenser and objective lens to form an incident electron beam with a certain energy and illumination intensity, and an extremely fine beam spot diameter. Under the action of a scanning coil, the electron beam performs a light like scan on the surface of the sample. The secondary electrons, backscattered electrons, and other signals excited in the sample are received by detection devices such as scintillators, and converted into optical signals. Then, they are amplified by a photomultiplier tube and converted into electrical signals. Finally, the signal data is processed by a computer to present the electronic coil image of the surface morphology of the sample on a display. In scanning electron microscopy, secondary electron images reflect the microstructure of the sample surface, while backscattered electron images are used to display the microstructure of some special biological samples.

Sample preparation: Under the conditions of vulcanization temperature of 165 °C, vulcanization pressure of 15 MPa, and vulcanization time of T90, the YXE-25D flat vulcanizing machine was used for vulcanization. The thickness of the vulcanized sample was 2.0 mm, the width of the sample was 6.0 mm, and the length was 25mm; Cut the vulcanized sample vertically with an ultrasonic cutting knife to obtain the sample; Fix the sample on the sample table with double-sided tape or conductive adhesive, and spray the sample with gold.

Experimental environment: Temperature: 20-23 °C.Relative humidity: 60%. Meets the anti-vibration and anti-magnetic requirements of FEI Teneo VS field emission electron microscope.

Operation steps:

(1) Using high-purity N2, release the vacuum state of the sample chamber and open it;(2) Install the sample stage carrying the sample on the carrier stage, record the position of the sample, close the sample chamber, and evacuate;(3) Adjust the position of the stage according to the placement of the sample;(4) After the vacuum degree reaches the working state, click Beamon to open the electron beam channel;(5) At low magnification, select an appropriate area of the sample, adjust the focal length, center the electron beam, eliminate image astigmatism, and take photos;(6) Under appropriate magnification, select the appropriate area of the sample, adjust the focal length, align the electron beam, eliminate image astigmatism, and take photos;(7) Replace other samples, adjust the focal length, align the electron beam, eliminate image astigmatism, and take photos;(8) After the shooting is completed, take out the sample and restore the sample chamber to a vacuum state.

2.4. Physical and chemical properties of micronized recycled rubber

The self-developed micro-nano reclaimed rubber has a particle size of approximately 239 nm, a sol content of 41.7-45%, and a gel content of 55-58.3%. Other physical and mechanical properties are listed in Table 2.

After oxidative degradation, rubber and carbon black (CB) can achieve dissociation. A portion of the rubber transforms into sol, while the remaining portion forms a gel primarily composed of carbon black. The micro-nano rubber-carbon black morphology in the gel is shown in Figure 2, and the CB particle size distribution is illustrated in Figure 3.

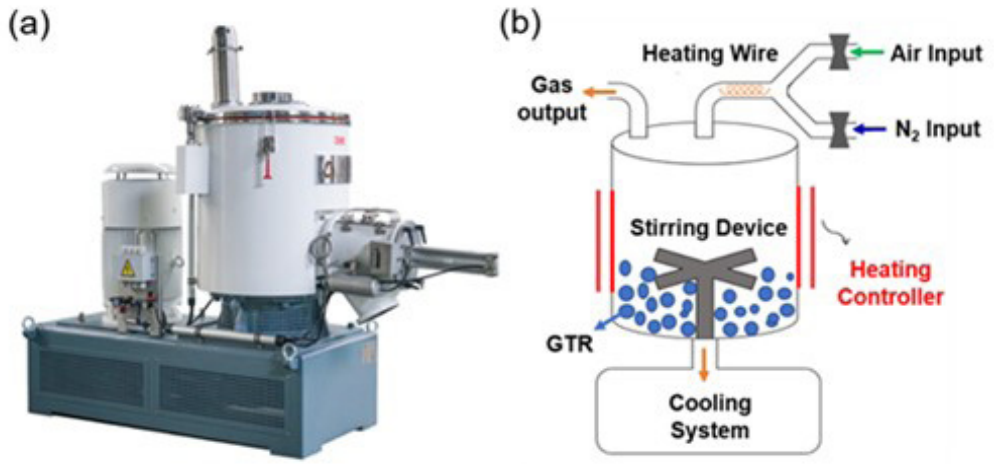

Figure 1. Homemade thermal oxidation reactor (a) Equipment diagram (b) Schematic diagram of equipment structure.

Table 2. Properties of micro-oxygenated micro-nano reclaimed rubber.

Project	Mooney viscosity	Sol content/%	Molecular weight of sol/(Mn/g/mol)	tensile strength/MPa	Elongation /%
Test result	40.8-42.5	41.7-45%	8866-10000	7-8	200-220%

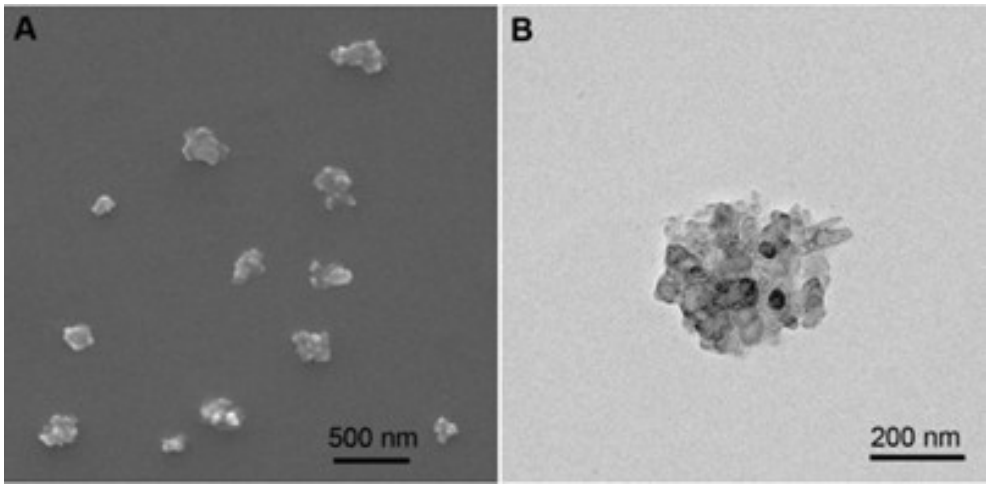

Figure 2. SEM (A) and TEM (B) of degraded micro-nano rubber of RGTR.

3. Method for Dispersion Identification

In the study of rubber filler dispersion, there is a considerable amount of research on carbon black filling[31,32]. Wang et al.[33] measured the micro-dispersion degree of carbon black in rubber by the distance from the center to the center of the filler and the distance from the boundary to the boundary. Moon et al.[34] studied the aggregation of carbon black in nitrile rubber using terahertz near-field microscopy. Akutagawa[35] used a nano-sized finite element method to improve the dispersion of carbon black in rubber compounds. Koga et al.[36] used Bonse-Hart type ultra-small angle neutron scattering (USANS) and Bonse-Hart type ultra-small angle X-ray scattering (USAXS), as well as small-angle X-ray scattering (SAXS) to quantitatively characterize the aggregates and agglomerates of CB particles loaded in rubber. Carbon black dispersity can measure the dispersibility of carbon black. Currently, the measurement of carbon black dispersion in China is governed by the national standard GB/T 6030-2006[37] "Rubber—Evaluation of carbon black and carbon black/silica dispersion—Quick comparison method," which specifies five measurement methods, four of which involve visual comparison with standard dispersion grade charts. The American Society for Testing and Materials has issued the ASTM D 2663[38] Standard Test Methods for Carbon Black—Dispersion in Rubber, which primarily relies on visual analysis for the measurement of carbon black dispersion in rubber, divided into five grades from 1 to 5. Lacayo-Pineda[39] classified the dispersion of fillers in rubber into three types: visual dispersion larger than 100 microns observable by the naked eye, macro dispersion from 2 microns to 100 microns observable by general instruments, and micro-dispersion below 2 microns that requires observation with an electron microscope or similar equipment.

In the filling of micro-nano regenerative rubber, due to the smaller size of the filler material, electron microscopy scanning is commonly used to obtain images of the filler distribution. However, electron microscopy scanning does not output dispersion measurements like carbon black dispersometers do. Moreover, visual methods require human resource investment and are subject to subjective factors,

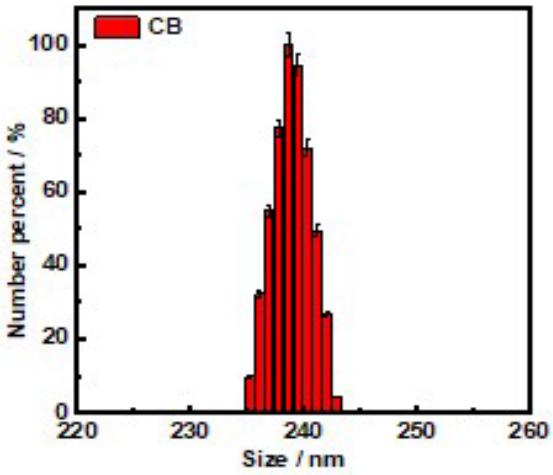

Figure 3. Size of degraded micro-nano rubber of RGTR.

making them difficult to use on a large scale and rapidly. Additionally, it is challenging to make subjective judgments on small and numerous particles. Based on this research motivation, this paper proposes a novel automated dispersion grading method for electron microscopy scanning images of micro-nano regenerative rubber filling.

3.1. Image preprocessing

Figure 4 shows the overall process of automatically identifying micro nano regenerated rubber in SEM images. We used MATLAB software programming to implement image reading, enhancement, and binarization operations, and applied functions from its image processing toolbox. The pixel-to-area conversion, labeling of large particle clusters, and calculation of dispersion were implemented by writing functions based on the formulas designed in the paper. First, the acquired electron microscope images are subjected to image enhancement, which improves the contrast, brightness, and color properties of the images, making them visually clearer and more vivid. This facilitates the observation and recognition of details

and features in the images. For machine vision and image processing systems, image enhancement techniques can make the features in the images more prominent and recognizable, thereby increasing the system's recognition rate and accuracy. Subsequently, binarization processing is carried out, which aims to convert grayscale or color images into binary images that contain only two levels of gray, representing black and white. This conversion greatly simplifies the image data and allows the target areas and background areas in the image to be clearly separated.

In some standards, agglomerates with a diameter ≥ 23μm are used as a reference for measuring dispersion. However, in actual mixing, the agglomerates are irregularly shaped. Therefore, this paper converts the pixels of the continuously connected filling area to equivalent circles, as shown in Figure 5a, where the green part, also known as the 8-connected component, consists of 8 pixels in the 8-neighborhood of the blue center pixel. A pixel and its 8-connected pixels are considered to be a continuous area if they have the same value on the binary image. As shown in Figure (b), the red area is considered to be continuously adjacent and is equivalent to the cluster in Figure (c). This allows the conversion of irregularly distributed micro-nano regenerated rubber into equivalent area circles with the same diameter. In this way, the areas of larger clusters can be identified.

3.2. Dispersion calculation

Subjective grading judgment is fraught with inconsistencies and inaccuracies due to the lack of objective standards, which also lacks objectivity and verifiability. Moreover, it is limited by the focus on specific features and the high cost in terms of time. Therefore, an objective and effective grading method that can be automatically calculated is particularly important for dispersion judgment. The previous section dealt with the equivalent conversion of pixel counts to circular areas. This section will convert the area of continuous pixels to the area of a circle with a diameter of 23μm, in order to mark large particles on the image and calculate the area size of each continuous filled area pixel. As shown in Figure 6, based on its scale of 50μm, the area s of a scanning electron microscope image is 414μm by 287μm, containing 1536 by 1025 pixels. Therefore, the size of each pixel is $spp = \frac{s}{1536*1025} = 0.075\text{i}\ \text{m}^2$, On a proportional diagram, the area of a circle with a diameter of 5μm is $s_c = \pi(\frac{5}{2})^2 = 19.635\mu\text{m}^2$. Consequently, it is possible to calculate the number of pixels in a continuous area on the scanning electron microscope image, multiply by the area of each pixel, and compare it with the area of a circle of a given diameter to obtain the number of regenerated rubber fillers within this threshold.

Following the steps in Figure 4, automated identification of regenerated rubber filler particles is performed on actual SEM images. As shown in Figure 6, it is an original SEM image where larger filler particles can be observed with the naked eye, but quantification and grading are difficult. Figure 7, on the other hand, shows a quantitative analysis based on theprocess in Figure 4. To obtain more reasonable quantitative indicators, this paper's method takes into account the size, number, and proportion of filler particles comprehensively. Specifically, the ratio of the filled area to the total image area is considered the main component for dispersion grading. More specifically, the ratio of the number of white area pixels to the total number of pixels in the image is considered an important indicator of dispersion. If the ratio exceeds 10%, it is counted as 10%, and if it does not exceed, it is counted as the actual value. At the same time, particles below 1μm are considered to be well-dispersed, and the proportion of these particles to the total number of fillers is taken into account.

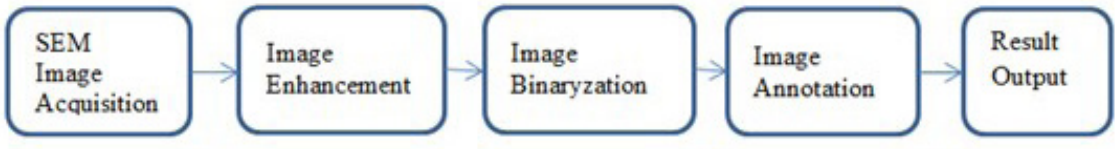

Figure 4. Diagram of the Image Processing Procedure.

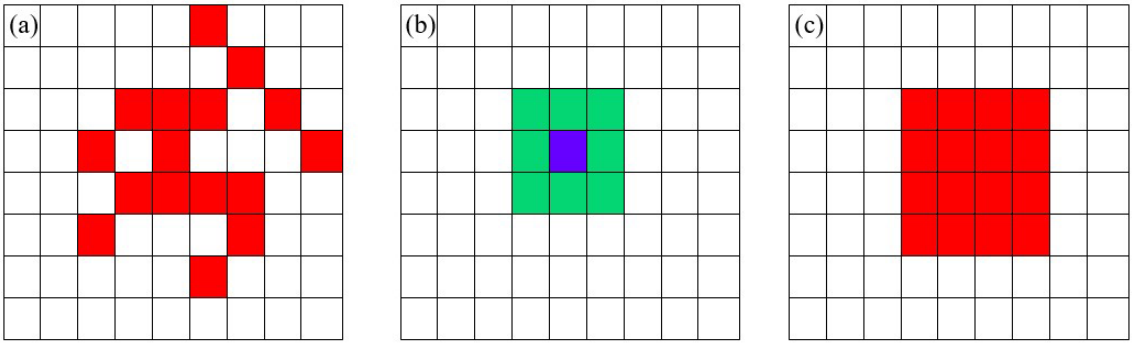

Figure 5. Schematic diagram of irregular cluster transformation.

6. Performance Metrics and Analysis

Automated measurement was conducted on the 8 formulations presented in Table 1, with the resulting indicator values shown in Table 3. The visualization results of recognition are shown in Figures 8, Figures 9, Figures 10, Figures 11, Figures 12, Figures 13, Figures 14, and Figures 15.

In the table, wpp represents the percentage of filler particle pixels to the total number of pixels. For values of wpp greater than 0.1, they will be calculated as 0.1. Tot is the number of filler clusters, Tow is the number of clusters less than 1μm, and Level is the final dispersion value. Its calculation method is as shown in Equation 1.

$$Level = 10 - wpp * 100 * \frac{Tow}{Tot} \tag{1}$$

The restriction on wpp ensures that the subtracted value does not exceed 10. While acknowledging the reinforcing effect of well-dispersed small particles on the material after filling, it also takes into account the negative impact of large particles.

Measurements of the mechanical properties of the rubber compounds were conducted, with the results shown in Table 4. To facilitate the presentation of correlations on the same order of magnitude, the data on a larger scale were scaled down and ultimately limited to a range of 0 to 10. This reduction does not affect the analysis results, as seen in Figure 16.

To analyze the relationship between the dispersion of micro-nano regenerated rubber and mechanical properties, the Pearson correlation coefficient r is introduced for analysis, with its range from -1 to 1. When r = 1, it indicates a perfect positive correlation between two variables; when r = -1, it indicates a perfect negative correlation. The definition is as shown in Equation 2.

$$\rho(A,B) = \frac{\mathrm{cov}(A,B)}{\sigma(A) * \sigma(B)} \tag{2}$$

In the formula, cov represents the covariance between two vectors, and σ represents the standard deviation. The

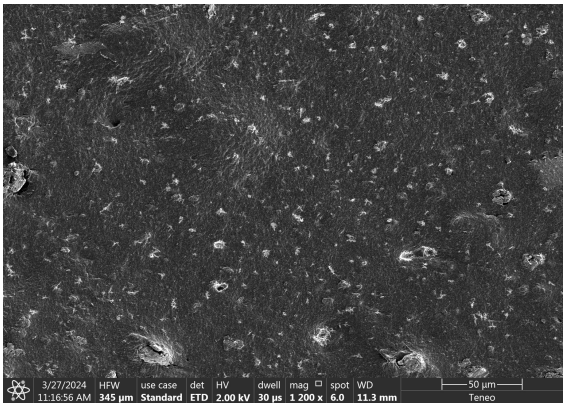

Figure 6. Scanning electron microscopy image of micro nano regenerated rubber filling.

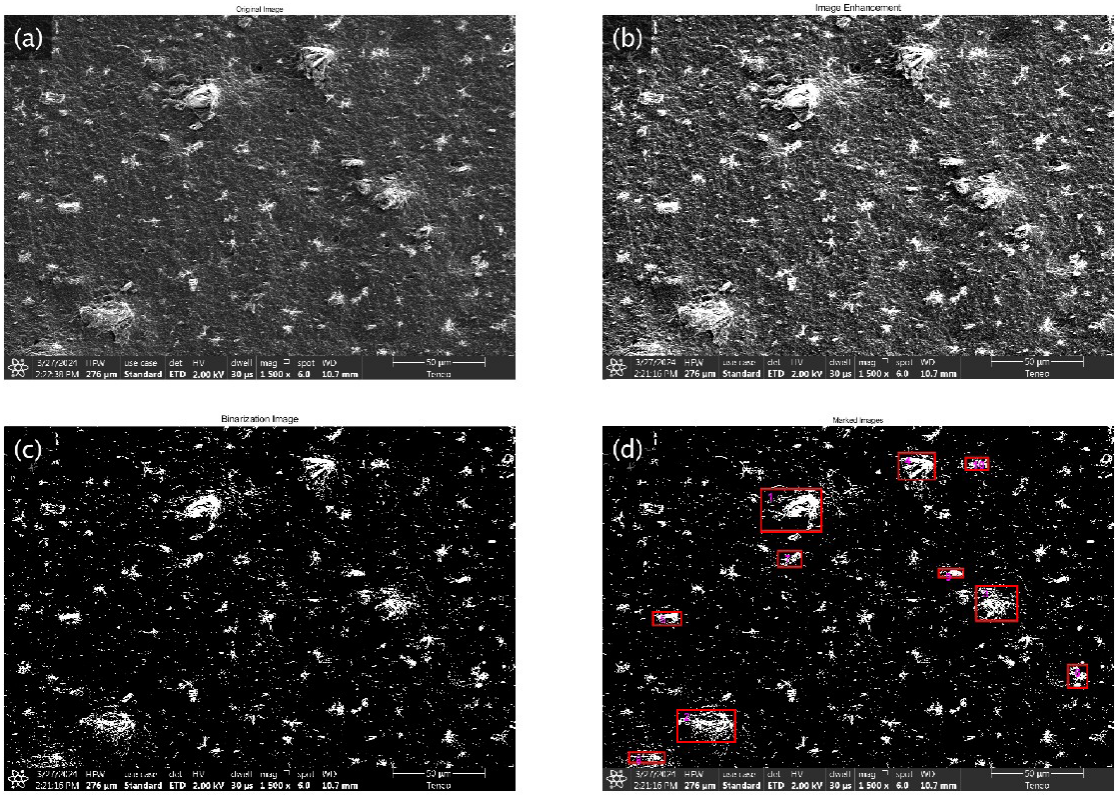

Figure 7. Example diagram of the method in this article, original image - image enhancement - binarization - large particle labeling.

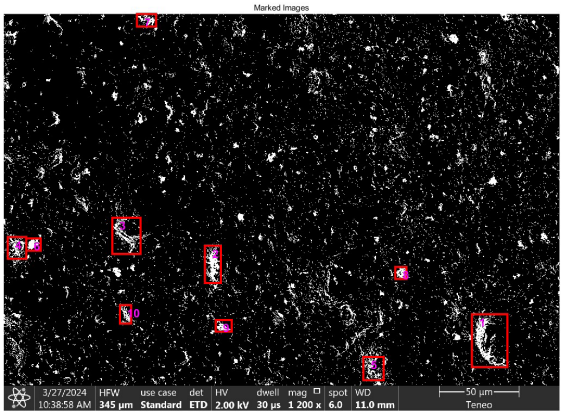

Figure 8. Measurement of Formula 1 #.

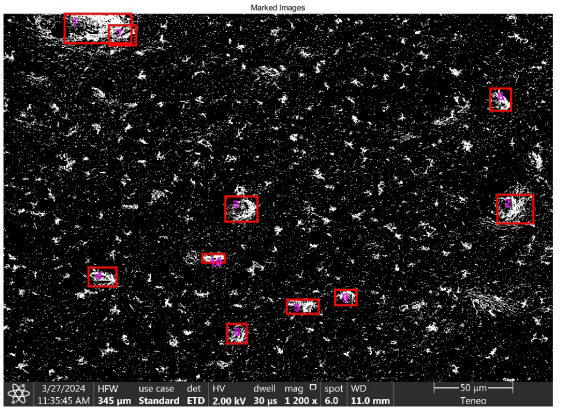

Figure 11. Measurement of Formula 4 #.

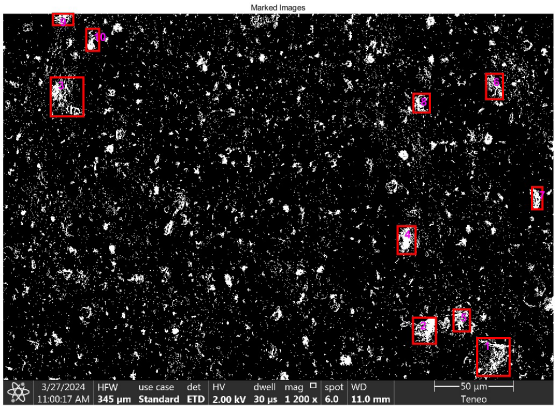

Figure 9. Measurement of Formula 2 #.

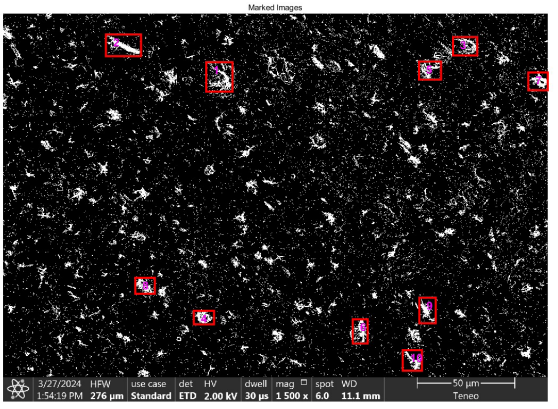

Figure 12. Measurement of Formula 5 #.

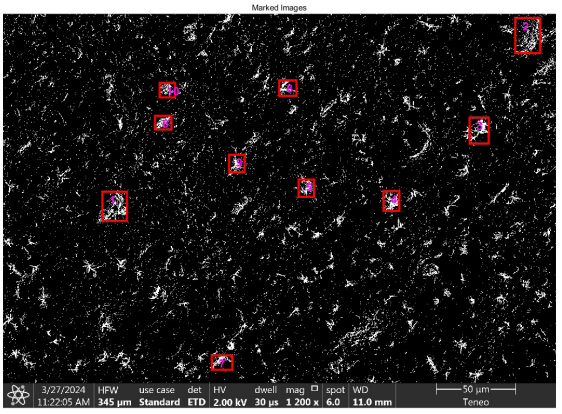

Figure 10. Measurement of Formula 3 #.

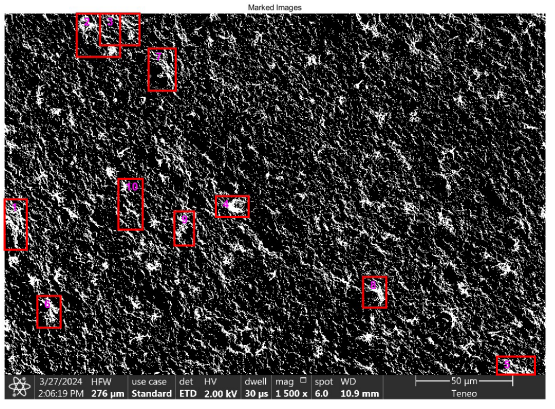

Figure 13. Measurement of Formula 6 #.

Pearson correlation coefficient between dispersion and tensile elongation at break is 0.846, with the coefficient for elongation at break being 0.938, for tear strength it is 0.766, for 300% modulus it is 0.836, for the modulus after aging at 300% it is 0.836, for the modulus after aging at 100% it is 0.750, for elongation at break after aging it is 0.708, for compression temperature it is -0.674, for air permeability it is -0.542, and for vulcanization performance (t90) it is -0.931. It can be seen that the micro-nano regenerated rubber dispersion assessment method proposed in this paper has a significant correlation with tensile elongation at break, elongation at break, modulus, and vulcanization performance.

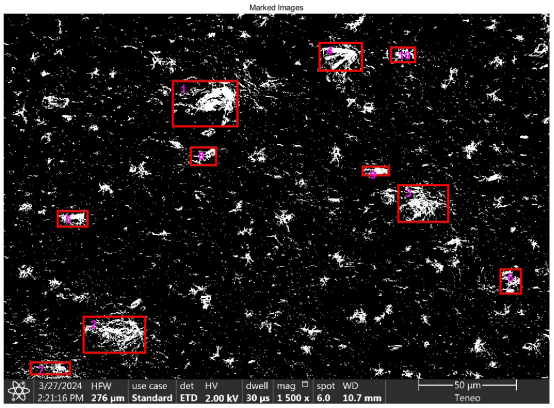

Figure 14. Measurement of Formula 7#.

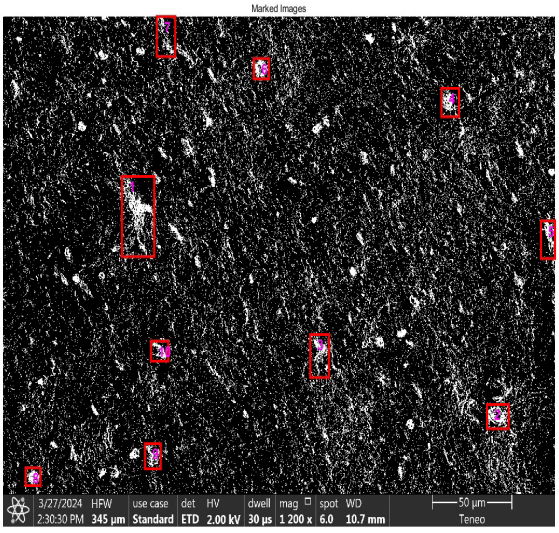

Figure 15. Measurement of Formula 8 #.

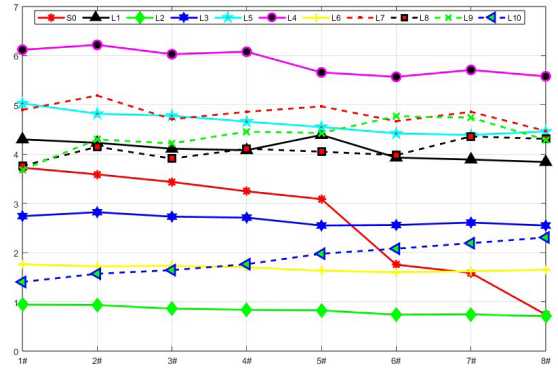

Figure 16. Distribution and mechanical properties of micro-nano regenerated rubber.

4.1. Correlation analysis between dispersion and mechanical properties

From the data in Table 4, it can be seen that as the filling amount of micro nano regenerated rubber increases (from 1 # to 8 #), the dispersibility index (Level) gradually decreases (3.72 → 0.70), indicating that the agglomeration phenomenon of the filler intensifies. At the same time, key mechanical performance indicators such as tensile strength (L1), elongation at break (L2), and tear strength (L3) of the material showed a decreasing trend (such as tensile strength decreasing from 9.43 MPa to 7.08 MPa). Pearson correlation analysis further confirmed the significant positive correlation between dispersion and these properties (r=0.846~0.938), indicating that the higher the dispersion, the more uniform the interface bonding between the filler and the matrix, and the higher the stress transfer efficiency, thereby enhancing the overall performance of the material. This result is consistent with literature[12,13]. The conclusion that "uniform dispersion can reduce stress concentration points" is consistent.

It is worth noting that the decrease in 300% tensile stress (L4) and aging tensile stress (L5) (6.12 → 5.58 MPa) is directly related to the decrease in dispersion, which may be due to the aggregation of fillers causing the cross-linking network to be blocked, weakening the elastic recovery ability of rubber. In addition, the compression temperature rise (L8) and air permeability (L9) are negatively correlated with dispersion (r=-0.674 and -0.542), indicating that poor dispersion can exacerbate internal friction and heat generation in materials. At the same time, uneven distribution of fillers can form permeation channels, reducing air tightness.

4.2. The influence of dispersion on sulfurization performance

The strong negative correlation between vulcanization time (t90) and dispersion (r=-0.931) indicates that the lower the dispersion, the slower the vulcanization reaction rate. This may be because the agglomerated fillers hinder the diffusion of the vulcanizing agent in the matrix, resulting in a decrease in the efficiency of crosslinking network formation. This discovery provides a theoretical basis for optimizing sulfurization process parameters such as temperature and pressure.

5. Influence of ZnO on SEM Image Contrast

The micro-nano regenerated rubber filler dispersion automatic grading method studied in this paper is analyzed using tire air barrier layer rubber as an example. The ZnO employed exhibits significant characteristics: a purity of 97.5%, fine particle size with an average of 60-70 nm, and a large specific surface area of 60-80 m^2/g. These properties influence the dispersion state of regenerated rubber and subsequent analyses.

5.1. Primary role of ZnO in rubber vulcanization

In rubber formulations, ZnO primarily acts as a vulcanization activator. The active ZnO used in tire air barrier layer formulations has high reactivity due to abundant surface -OH and Zn^{2+} groups. During vulcanization, these groups rapidly react with sulfur (S), accelerator TMTD, and accelerator DM. The -OH groups form hydrogen bonds with polar groups on rubber molecular chains, enhancing chemical bonding strength, crosslink network density, and mechanical properties (e.g., tensile strength and tear resistance). Concurrently, Zn^{2+} ions undergo complexation with sulfur and accelerators to form reactive intermediates,

Table 3. Dispersion Metrics and Grading Table.

	1#	2#	3#	4#	5#	6#	7#	8#
wpp	0.0677	0.0699	0.0691	0.0711	0.0788	0.1714	0.0867	0.1306
Tot	20067	18777	23199	23200	24560	21519	12562	44463
Tow	18602	17224	22043	22043	21549	17745	12192	41358
Level	3.72	3.59	3.43	3.24	3.09	1.75	1.59	0.70

Table 4. Relationship between Dispersion and Mechanical Properties.

Number	Ingredient formula	1#	2#	3#	4#	5#	6#	7#	8#
S0	Dispersion value	3.72	3.59	3.43	3.24	3.09	1.75	1.59	0.70
L1	Tensile strength /MPa	9.43	9.33	8.6	8.37	8.25	7.37	7.43	7.08
L2	Elongation at break /%	430	423	411	408	439	393	389	384
L3	Tear strength KN/m	27.4	28.2	27.3	27.1	25.5	25.6	26.1	25.5
L4	300% Tensile stress	6.12	6.22	6.03	6.08	5.66	5.57	5.71	5.58
L5	300% Tensile stress after aging	5.03	4.82	4.78	4.66	4.55	4.42	4.39	4.46
L6	100% Tensile stress after aging	1.76	1.72	1.73	1.7	1.63	1.6	1.62	1.65
L7	Elongation at break after aging	490	519	471	486	497	467	486	447
L8	Compression temperature	37.6	41.5	39.1	41.1	40.5	39.8	43.6	43.1
L9	Breathability $cm^3/m^2.24h.0.1MPa$	36.82	42.98	42.17	44.58	44.28	47.70	47.42	42.90
L10	Sulfurization performance 90/s	1403	1570	1643	1764	1977	2079	2191	2307

accelerating vulcanization. Additionally, Zn^{2+} coordinates with functional groups on rubber chains, further improving crosslinking degree, heat resistance, and aging resistance. The formulation studied has been applied in the air barrier layer of radial engineering tires at Xuzhou Xulun Rubber Co., Ltd., demonstrating satisfactory mechanical properties, heat resistance, aging resistance, and moderate vulcanization speed, confirming the rationality of using 10 phr active ZnO as a vulcanization activator.

5.2. Potential impact of ZnO electronic properties on SEM image contrast

5.2.1. Electronic characteristics of ZnO

ZnO is a wide-bandgap semiconductor, and its electronic properties (e.g., charge transport and distribution) may influence SEM imaging. Variations in ZnO crystal structure or surface properties could lead to uneven charge distribution, manifesting as gray-level differences in images and affecting contrast.

5.2.2. Light absorption and scattering effects of ZnO

ZnO exhibits specific optical properties, including light absorption and scattering within certain wavelength ranges. In imaging systems, ZnO in the medium may alter light propagation and distribution. When incident light interacts with ZnO-containing regions, partial absorption or scattering occurs, resulting in localized intensity variations and contrast differences.

5.3. Impact of ZnO vulcanization property changes on SEM image contrast

5.3.1. Potential effects of altered ZnO vulcanization properties

During vulcanization, sulfur atoms may react with Zn atoms on ZnO surfaces to form compounds such as zinc sulfide (ZnS). ZnS formation could modify surface roughness and chemical activity, thereby altering ZnO's optical and electronic properties and indirectly influencing image contrast.

5.3.2. Influence of ZnO dispersion uniformity on SEM image contrast

Non-uniform ZnO distribution in the rubber matrix may lead to heterogeneous vulcanization, causing variations in material properties (e.g., mechanical strength, heat resistance, and air-tightness). Such heterogeneity may translate into optical property differences across regions, resulting in contrast variations during imaging.

5.3.3. Impact of filler aggregation on SEM image contrast

Interactions between ZnO and the vulcanization system may influence filler aggregation. On one hand, sulfides formed on ZnO surfaces could alter wettability and charge distribution, affecting filler-filler interactions. For instance, hydrophilic or hydrophobic surface modifications may promote filler aggregation. On the other hand, crosslinked networks generated during vulcanization may restrict ZnO particle mobility, enhancing aggregation. Aggregated fillers induce localized optical heterogeneity, thereby impacting image contrast.

The analysis reveals that ZnO not only serves as a vulcanization activator but also subtly influences SEM image contrast. As shown in Table 4, minimal fluctuations in mechanical properties, heat resistance, air-tightness, and vulcanization performance across formulations indicate uniform ZnO dispersion and negligible filler aggregation during vulcanization, suggesting limited impact on SEM image contrast.

6. Conclusion

In this study, we explored the impact of the dispersion of micro-nano regenerated rubber on the mechanical properties of composite materials. By introducing an automated assessment method based on scanning electron microscopy (SEM) images, we were able to objectively quantify the dispersion of micro-nano regenerated rubber, providing a precise and effective alternative to traditional subjective evaluations. This method not only enhances the accuracy of assessments but also contributes to the sustainable development of materials. Our research findings indicate that the dispersion of micro-nano regenerated rubber has a significant correlation with various mechanical performance indicators of composite materials, such as elongation at break, tensile strength, modulus, and vulcanization performance. Additionally, we found that dispersion is negatively correlated with certain performance metrics, such as compression temperature and air permeability, offering new insights for further optimizing material performance. Looking ahead, we plan to apply this automated assessment method for real-time monitoring and extend it to other types of filling systems, aiming to further enhance the performance of composite materials and advance technological progress in related fields.

The practical significance of this study lies in:Environmental protection and resource utilization: Micro nano regenerated rubber does not require the addition of polluting chemicals such as coal tar, which meets the needs of green circular economy. Industrial application prospects: Automated evaluation methods can be integrated into real-time monitoring systems for rubber mixing processes, assisting in the development of high-performance composite materials.

Future work will focus on:Multi material system extension: Verify the applicability of the method in silicon-based fillers, nanoclay, and other systems. Algorithm optimization: Introducing deep learning (such as U-Net segmentation model) to improve the recognition accuracy of ultra micron sized fillers. Dynamic process research: Combining rheology and in-situ SEM technology to reveal the dynamic mechanism of dispersion evolution during mixing process. Use other techniques to validate and improve data, test and validate this method. Systematically explore the effects of ZnO types (e.g., indirect-method ZnO, active ZnO) and dosage variations on SEM image contrast, providing deeper theoretical insights for automated micro-nano filler dispersion grading methods.

7. Acknowledgments

The work is supported by the National Natural Science Foundation of China, Mechanism and Application of Oxygen-Supply-Regulated Low-Temperature Efficient Mild Cracking of Rubber Powder (52173103). Jiangsu Province Higher Education Institutions Fundamental Research Program of Natural Science, Micro-Oxygen Micro-Nano Recycling of Waste Rubber and Its High-Value Application in Tires (23KJA430015).

8. References

1. Chittella H, Yoon LW, Ramarad S, Lai Z-W. Rubber waste management: a review on methods, mechanism, and prospects. Polym Degrad Stabil. 2021;194:109761. http://doi.org/10.1016/j.polymdegradstab.2021.109761.
2. Amjad-Iranagh S, Alinejad N. Sustainability approach for nanofillers in additives for rubber and tire industry. In: Mallakpour S, Hussain CM, editors. Handbook of nanofillers. Singapore: Springer; 2024. http://doi.org/10.1007/978-981-99-3516-1_95-1.
3. Mei J, Xu G, Ahmad W, Khan K, Amin MN, Aslam F, et al. Promoting sustainable materials using recycled rubber in concrete: a review. J Clean Prod. 2022;373:133927. http://doi.org/10.1016/j.jclepro.2022.133927.
4. Jalali SK, Busfield J, Pugno N. Micromechanics model for rubber blends filled by a nano-reinforced devulcanized recycled rubber: application in the automotive industry. Int J Automot Technol. 2023;24(4):983-94. http://doi.org/10.1007/s12239-023-0080-z.
5. Leong S-Y, Lee S-Y, Koh T-Y, Ang DT-C. 4r of rubber waste management: current and outlook. J Mater Cycles Waste Manag. 2023;25(1):37-51. http://doi.org/10.1007/s10163-022-01554-y. PMid:36466440.
6. Asaro L, Gratton M, Seghar S, Hocine NA. Recycling of reshubber wastes by devulcanization Resour. Resour Conserv Recycling. 2018;133:250-62. http://doi.org/10.1016/j.resconrec.2018.02.016.
7. Stock V, Böhmert L, Coban G, Tyra G, Vollbrecht M-L, Voss L, et al. Microplastics and nanoplastics: size, surface and dispersant – what causes the effect? Toxicol In Vitro. 2022;80:105314. http://doi.org/10.1016/j.tiv.2022.105314. PMid:35033651.
8. Hou C, Song X, Tang F, Li Y, Cao L, Wang J, et al. W–Cu composites with submicron- and nanostructures: progress and challenges. NPG Asia Mater. 2019;11(1):74. http://doi.org/10.1038/s41427-019-0179-x.
9. Jalali SK, Busfield J, Pugno N. Micromechanics model for rubber blends filled by a nano-reinforced devulcanized recycled rubber: application in the automotive industry. Int J Automot Technol. 2023;24(4):983-94. http://doi.org/10.1007/s12239-023-0080-z.
10. Glaskova T, Zarrelli M, Borisova A, Timchenko K, Aniskevich A, Giordano M. Method of quantitative analysis of filler dispersion in composite systems with spherical inclusions. Compos Sci Technol. 2011;71(13):1543-9. http://doi.org/10.1016/j.compscitech.2011.06.009.
11. Thiem J, Cole DP, Dubey U, Srivastava A, Ashraf C, Henry TC, et al. Using data science to locate nanoparticles in a polymer matrix composite. Compos Sci Technol. 2022;218:109205. http://doi.org/10.1016/j.compscitech.2021.109205.
12. Nishi T. Rubber wear mechanism discussion based on the relationship between the wear resistance and the tear resistance

with consideration of the strain rate effect. Wear. 2019;426-427:37-48. http://doi.org/10.1016/j.wear.2018.12.084.
13. Guchait A, Saxena A, Chattopadhyay S, Mondal T. Influence of nanofillers on adhesion properties of polymeric composites. ACS Omega. 2022;7(5):3844-59. http://doi.org/10.1021/acsomega.1c05448. PMid:35155882.
14. Liu L, Zhang D, Zhu Y, Han Y. Bulk and local structures of metal–organic frameworks unravelled by high-resolution electron microscopy. Commun Chem. 2020;3(1):99. http://doi.org/10.1038/s42004-020-00361-6. PMid:36703329.
15. Attia D, Cohen SM, Levi-Kalisman Y, Bitton R, Yerushalmi-Rozen R. Ph-responsive re-dispersible dispersions of carbon black and single-walled carbon nanotubes in arabinogalactan solutions. J Mol Liq. 2025;419:126786. http://doi.org/10.1016/j.molliq.2024.126786.
16. Chang C-W, Yen Y-S, Lai C-H, Li C-C. Optimized dispersion and alignment of iron particles in magnetic composite films. Mater Chem Phys. 2025;334:130397. http://doi.org/10.1016/j.matchemphys.2025.130397.
17. Li Z, Gao Y, Moon K-S, Yao Y, Tannenbaum A, Wong CP. Automatic quantification of filler dispersion in polymer composites. Polymer (Guildf). 2012;53(7):1571-80. http://doi.org/10.1016/j.polymer.2012.01.048.
18. Xu Z, Song Y, Zheng Q. Payne effect of carbon black filled natural rubber compounds and their carbon black gels. Polymer (Guildf). 2019;185:121953. http://doi.org/10.1016/j.polymer.2019.121953.
19. Łapińska A, Grochowska N, Antonowicz J, Michalski P, Dydek K, Dużyńska A, et al. Influence of the filler distribution on pdms-graphene based nanocomposites selected properties. Sci Rep. 2022;12(1):19038. http://doi.org/10.1038/s41598-022-23735-3. PMid:36352248.
20. Demir EC, McDermott MT, Kim CL, Ayranci C. Towards better understanding the stiffness of nanocomposites via parametric study of an analytical model modeling parameters and experiments. J Compos Mater. 2023;57(6):1087-104. http://doi.org/10.1177/00219983221149122. PMid:36974194.
21. Zhou J, Hou D, Cheng S, Zhang J, Chen W, Zhou L, et al. Recent advances in dispersion and alignment of fillers in PVDF-based composites for high-performance dielectric energy storage. Mater Today Energy. 2023;31:101208. http://doi.org/10.1016/j.mtener.2022.101208.
22. Wei H, Lv X, Zhao Y, Li C, Yan H, Sun R, et al. Quantitative description of filler dispersion in composite materials by fractal analysis and fluorescent labeling-LSCM visualization technology. Polym Compos. 2022;43(6):3598-608. http://doi.org/10.1002/pc.26640.
23. Xu Y, Wang S, Haq ZU, Ren T, Luo Z, Tu H, et al. The preparation of different types of reclaimed rubber and their applications in tire inner liner. J Appl Polym Sci. 2024
24. ISO: International Organization for Standardization. ISO 6502:1991: rubber: measurement of vulcanization characteristics with rotorless curemeters. Geneva: ISO; 1991.
25. ASTM: American Society for Testing and Materials. ASTM D7723-11: standard test method for rubber property—macro-dispersion of fillers in compounds. West Conshohocken: ASTM; 2011.
26. National Standards of the People's Republic of China. GB/T 528-2009: determination of tensile stress-strain properties of vulcanized rubber or thermoplastic rubber. Shenzhen: GB; 2009.
27. National Standards of the People's Republic of China. GB/T 529-2008: determination of tear strength of vulcanized rubber or thermoplastic rubber. Shenzhen: GB; 2008.
28. National Standards of the People's Republic of China. GB/T 3512-2014: vulcanized rubber or thermoplastic rubber: accelerated aging and heat resistance tests. Shenzhen: GB; 2014.
29. ISO: International Organization for Standardization. ISO 4666-3:2010: rubber, vulcanized: determination of temperature rise and resistance to fatigue in flexometer testing—part 3: compression flexometer (constant-strain type). Geneva: ISO; 2010.</bok>
30. ISO: International Organization for Standardization. ISO 2782:1995: rubber, vulcanized or thermoplastic: determination of permeability to gases. Geneva: ISO; 1995.
31. Fan Y, Fowler GD, Zhao M. The past, present and future of carbon black as a rubber reinforcing filler – a review. J Clean Prod. 2020;247:119115. http://doi.org/10.1016/j.jclepro.2019.119115.
32. Persson S. Dispersion of carbon black. Polym Test. 1984;4(1):45-59. http://doi.org/10.1016/0142-9418(84)90032-1.
33. Wang CC, Wu SH, Donnet JB, Wang TK. Microdispersion of carbon blacks in rubber : distance distribution of aggregates by afm image analysis part II. KGK Kautsch Gummi Kunstst. 2006;59(9):466-72.
34. Moon Y, Lee H, Jung J, Han H. Direct visualization of carbon black aggregates in nitrile butadiene rubber by thz near-field microscope. Sci Rep. 2023;13(1):7846. http://doi.org/10.1038/s41598-023-34565-2. PMid:37188716.
35. Akutagawa K. Technology for reducing tire rolling resistance. Tribology Online. 2017;12(3):99-102. http://doi.org/10.2474/trol.12.99.
36. Koga T, Takenaka M, Aizawa K, Nakamura M, Hashimoto T. Structure factors of dispersible units of carbon black filler in rubbers. Langmuir. 2005;21(24):11409-13. http://doi.org/10.1021/la051352s. PMid:16285818.
37. National Standards of the People's Republic of China. GB/T 6030-2006: rubber: evaluation of carbon black and carbon black/silica dispersion: quick comparison method. Shenzhen: GB; 2006.
38. ASTM: American Society for Testing and Materials. ASTM D2663: standard test methods for carbon black—dispersion in rubber. West Conshohocken: ASTM; 2019.
39. Lacayo-Pineda J. Filler dispersion and filler networks. In Kobayashi S, Müllen K, editors. Encyclopedia of polymeric nanomaterials. Berlin: Springer; 2015. p. 771-76. http://doi.org/10.1007/978-3-642-29648-2_291.

Data availability

The entire dataset supporting the results of this study has been made available on SciELO Data and can be accessed at [https://github.com/too007007/mr-2024-0493_enviadoAutor/tree/main].